JOURNAL OF AGRICULTURAL AND FOOD CHEMISTRY

ARTICLE

pubs.acs.org/JAFC

Profiling of Resveratrol Oligomers, Important Stress Metabolites, Accumulating in the Leaves of Hybrid *Vitis vinifera* (Merzling × Teroldego) Genotypes Infected with *Plasmopara viticola*

Fulvio Mattivi,*[,†] Urska Vrhovsek,[†] Giulia Malacarne,[†] Domenico Masuero,[†] Luca Zulini,[†] Marco Stefanini,[†] Claudio Moser,[†] Riccardo Velasco,[†] and Graziano Guella[‡]

[†]Fondazione Edmund Mach, IASMA Research and Innovation Centre, Via E. Mach 1, 38010 San Michele all'Adige, Italy

[‡]Laboratory of Bioorganic Chemistry, Department of Physics, University of Trento, Via Sommarive 14, 38050 Povo, Trento, Italy

Supporting Information

ABSTRACT: In the Vitaceae, viniferins represent a relatively restricted group of *trans*-resveratrol oligomers with antifungal properties, thus enabling plants to cope with pathogen attack. The aim of this study was to perform isolation and structural characterization of the whole class of viniferins accumulating in the leaves of hybrid *Vitis vinifera* (Merzling × Teroldego) genotypes infected with *Plasmopara viticola*. Infected leaves of resistant plants were collected 6 days after infection, extracted with methanol, and prepurified by flash chromatography using ENV+ and Toyopearl HW 40S resins. Further fractionation using normal-phase preparative chromatography and then reversed-phase preparative chromatography allowed isolation of 14 peaks. The isolated compounds were identified using advanced mass spectrometry techniques and extensive one- and two-dimensional nuclear magnetic resonance measurements, UV, CD, optical properties, and molecular mechanic calculations. The results demonstrated the presence in infected leaves of seven dimers (six stilbenes and one stilbenoid), of which four were new in grapevine (ampelopsin D, quadrangularin A, *E*-ω-viniferin, and *Z*-ω-viniferin), four trimers (three stilbenes and one stilbenoid), of which two (*Z*-miyabenol C and *E*-*cis*-miyabenol C) were new in grapevine, three tetramer stilbenoids, all new in grapevine, isohopeaphenol, ampelopsin H, and a vaticanol C-like isomer. The isolation of a dimer deriving from the condensation of (+)-catechin with *trans*-caffeic acid also indicated that other preformed phenolics are structurally modified in tissues infected with *P. viticola*.

KEYWORDS: *Vitis vinifera*, *Plasmopara viticola*, stilbenes, stilbenoids, NMR, mass spectrometry

INTRODUCTION

Within the Vitaceae, viniferins represent a relatively restricted group of low molecular weight phenolics consisting of *trans*-resveratrol derivatives with antifungal properties, thus enabling plants to cope with pathogen attack.[1] In the grapevine resveratrol production leads to the formation of phytoalexins deriving from oxidative oligomerization, called viniferins.[2] Some of these have been found to act biologically against various fungal pathogens in the grapevine.[3,4] The toxicity of stilbene phytoalexins for fungi was found to be closely related to their chemical structure. In particular, it was found that δ-viniferin, an oxidative resveratrol dimer, and pterostilbene, the 3,5-dimethoxy analogue of resveratrol, are the most toxic stilbenes against mobility and disease development of the oomycete *Plasmopara viticola*.[2,5]

Since the pioneering studies of Langcake and Pryce,[3] which elucidated the structure of *trans*-resveratrol, α-viniferin, and ε-viniferin, observing the presence of other uncharacterized viniferin-like compounds characteristic of the Vitaceae family, such as β-viniferin and γ-viniferin, and the formation of a *trans*-resveratrol dehydrodimer by horseradish peroxidase and H_2O_2 (later named δ-viniferin), there has been little progress in the structural characterization of this particular class of inducible bioactive compounds in vine leaves. Other stilbenes identified in leaves infected with *P. viticola* are the monomer pterostilbene[2] and the dimer δ-viniferin (synonym: *trans*-resveratrol dehydrodimer), reported to be the major viniferin synthesized in *P. viticola* infected and UV-irradiated *Vitis vinifera* var. Chasselas leaves,[5] whereas the stilbenoid α-viniferin has never been reported in subsequent studies. Most studies available to date have focused on the presence and functional role of these known structures, concentrating more on grape oligomers bearing the stilbenic double bond (oligostilbenes)[1,6] rather than on other stilbenoids.

This study was a part of a broader investigation aiming to establish the role of the whole class of viniferins in grapevine defense against *P. viticola*. A preliminary HPLC-DAD-MS screening showed that 17% of individuals in a segregating population (Merzling × *Vitis vinifera* Teroldego) display a high amount and a complex profile of known and unknown grapevine viniferins as compared to parental lines, following *P. viticola* infection.

The main aim of the present study was therefore to perform complete isolation and structural characterization of these viniferins from infected leaves of selected genotypes of the population resistant to *P. viticola*. The 10 major viniferins, as well as 3 other minor viniferins and 1 phenolic dimer present in infected leaves, were identified using advanced mass spectrometry

Received: February 24, 2011
Revised: April 21, 2011
Accepted: April 22, 2011
Published: April 22, 2011

techniques (LC-ESI-MS and LC-ESI-Q-TOF) and extensive one- and two-dimensional nuclear magnetic resonance (NMR) measurement, UV, CD, and optical properties. Molecular mechanics (MM) calculations were also carried out on all of the compounds reported here to find the most stable conformation.

MATERIALS AND METHODS

Grapevines. For isolation of the viniferins, 18 genotypes were chosen from the experimental vineyard of the Edmund Mach Foundation, in San Michele all'Adige, Italy, from an F1 population deriving from a cross between Merzling, a complex hybrid of *V. vinifera* descending from *V. rupestris* and *V. lincecumii*, and *V. vinifera* cv. Teroldego. The 10 apical leaves of 2−3 shoots were infected with *P. viticola*, sampled after 6 days, pooled, weighed (517 g), and stored at −20 °C.

Plant Infection. Sporangiospores of *P. viticola* (Berk. and Curt) Berl. et De Toni were collected from the infected leaves of *V. vinifera* cv. Pinot gris plants. The white mold emerging on the underside of the leaves was brushed into cold bidistilled water to obtain a conidial suspension of 10^4−10^5 spores/mL. Infection on plants was carried out by spraying the cold conidial suspension onto the lower surface of all fully expanded leaves in a climate chamber at 24 °C and 80% relative humidity.

Chemicals. Acetonitrile, methanol, and acetic acid were of HPLC grade and purchased from Carlo Erba (Milan, Italy), ethyl acetate was from BDH, and phosphoric acid was from Merck (Milan, Italy). Water was of Milli-Q grade. *trans*-Resveratrol and *trans*-4-hydroxystilbene were from Sigma-Aldrich (Milan, Italy), *cis*-Resveratrol was prepared from the standard of *trans*-resveratrol using photoisomeriszation, and *trans*-piceid (*trans*-resveratrol-3-*O*-β-D-glucopyranoside) was isolated from the dried roots of *Polygonum cuspidatum*.[7] The purity of each resveratrol monomer was controlled using HPLC, and identities were confirmed according to the method of Mattivi et al.[8]

Extraction. The process was done under nitrogen, in the dark and without mineral acids, to prevent the production of artifacts due to oxidation, photoisomerization, and hydrolysis. The leaves (517 g) were weighed, ground, and extracted for 48 h at room temperature in methanol (10 L). The solid material was removed and the volume of the extract reduced to 500 mL in a rotary evaporator at 35 °C.

Preparative Chromatography. Both low-pressure flash chromatography and high-pressure liquid chromatography were carried out on a preparative HPLC system (Shimadzu Corp., Kyoto, Japan) SCL-10 AVP model with two 8A pumps and a UV−vis detector (SPD-10 AVP), controlled via Software Class VP.

To guide extraction, both the crude extract and each of the intermediate fractions were analyzed using HPLC-DAD-MS.

Isolute ENV+ Flash Chromatography. The first step in extract cleanup was carried out with a 150 mL Isolute syringe column for flash chromatography, packed with 20 g of ENV+ bulk Isolute sorbent with a diameter of 40−70 μm and an average pore size of 60 μm, closed at both ends with Isolute SPE disk accessories (all from International Sorbent Technology Ltd., Hengoed, U.K.). The resin was activated before each use with sequential elution with methanol (200 mL) and water (300 mL). The crude extract was divided into two fractions, each fraction (250 mL) filtered on Durapore 0.22 μm (Millipore, Bedford, MA), absorbed on ca. 10 g of activated resin, and brought to dryness under reduced pressure. The resin was suspended in water and packed onto the syringe column, which was then inserted online in the HPLC system. Flash chromatography was carried out at room temperature with a flow of 25 mL/min and sequential elution with (A) water (350 mL), (B) pentane/dichloromethane 2:1 v/v (2 L), (C) ethyl acetate (500 mL), and (D) methanol (500 mL). Fractions B, C, and D were brought to dryness, redissolved with 50 mL of methanol, and analyzed using HPLC-DAD-MS. Fraction C contained all of the target compounds and was selected for further processing, whereas the others were discarded.

HW40S Flash Chromatography. A second cleanup was carried out using the same equipment, using 20 g of HW40S (Toyopearl) resin as a stationary phase. The methanol solution (fraction 3 from the purification with ENV+) was quantitatively loaded onto the syringe column. The column was inserted online onto the preparative HPLC, washed with water (500 mL) at 10 mL/min, and connected to the detector. The UV signal was acquired at 280 nm. Mobile phases consisted of water (A) and methanol (B). The chromatographic run consisted of a linear gradient from 50 to 100% B in 60 min and then isocratic 100% B for 40 min, with a flow of 10 mL/min. Sequential fractions of 50 mL were collected, and an aliquot of each was injected into the HPLC-DAD-MS to check composition. The fractions eluted from 50 to 90 min contained all of the stilbenes and stilbenoids. These were pooled, brought to dryness, and dissolved in 100 mL of methanol. This purified fraction was further enriched in the target compounds.

Preparative Normal-Phase HPLC. A Develosil 100DIOL-5, 300 × 20 mm, diol column (CPS Analitica, Milan, Italy) was chosen for fractionation of the different oligomers. The column was conditioned with acetonitrile, at a flow of 20 mL/min, and connected to a detector operating at 280 nm. Aliquots of 10 mL of the methanolic fraction containing the stilbenes were brought to dryness and dissolved in 0.5 mL of methanol and 0.5 mL of acetone before injection.

Chromatographic separation was carried out at room temperature in 65 min, with acetonitrile (A) and methanol mobile phases with 3% water (B). The profile was 100% A for 15 min, linear gradient to 15% B in 30 min, linear gradient to 100% B in 10 min, and hold at 100% B for 10 min. Each peak was separately collected, brought to dryness, dissolved in 10 mL of methanol, and analyzed using HPLC-DAD-MS. The seven fractions containing the stilbenes were brought to 1.5 mL in acetone for initial characterization using NMR.

Preparative Reversed-Phase Chromatography. A Discovery HS-C18 column, 250 × 21.2 mm, 5 μm (Supelco), was conditioned with water, with a flow of 10 mL/min and connected to a detector operating at 280 nm. Each of the seven fractions was brought to dryness, dissolved in 0.5 mL of methanol, and filtered with Durapore 0.22 μm (Millipore) before injection. Chromatographic separation was carried out at room temperature, in 78 min, with water (solvent A) and acetonitrile (B), with the following profile: 100% A for 3 min, followed by isocratic run at (30−27−32−34−32−32−32% B, variable according to the fraction 1−7) for 65 min, and hold at 100% B for 10 min. Each peak (14 in total) was separately collected, brought to dryness, dissolved in 10 mL of methanol, and analyzed using HPLC-DAD-MS.

HPLC-DAD-MS Analysis. These conditions were used to monitor each step in the isolation and were further validated to allow metabolite profiling of infected vines. Analysis took place on a Micromass ZQ LC-MS system (Micromass, Manchester, U.K.), equipped with a Waters 2690 HPLC system, a Waters 996 DAD detector (Waters Corp., Milford, MA), and Empower software (Waters Corp). Separation was performed using a Zorbax SB-Aq column, 5 μm, 2.1 × 150 mm (Agilent Technologies, Palo Alto, CA), and a Zorbax SB-Aq precolumn, 5 μm, 2.1 × 12.5 mm (Agilent Technologies). The mobile phases consisted of 0.1% acetic acid in H_2O (A) and acetonitrile (B). Separation was carried out at 40 °C in 27 min, under the following conditions: linear gradient starting at 5% B, to 70% B in 25 min, to 95% B in 0.1 min, 95% B for 2 min, and back to 5% B in 0.1 min. The column was equilibrated for 7 min prior to each analysis. The flow rate was 0.25 mL/min and the injection volume 6 μL. The UV−vis spectra were recorded from 220 to 400 nm, with detection at 280 and 310 nm.

Capillary voltage was 3000 V; cone voltage, 40 V; extractor voltage, 6 V; source temperature, 105 °C; desolvation temperature, 200 °C; cone gas flow (N_2), 30 L/h; and desolvation gas flow (N_2), 450 L/h. The outlet of the HPLC system was split (9:1) to the ESI interface of the

Table 1. Name, Amount Isolated, and MS Data of the Compounds Obtained from *P. viticola* Infected Grapevine Leaves

fraction	retention time (min)	amount (mg)	size	name	molecular formula	MM calculated	molecular ion $(M-H)^-$	observed $(M-H)^-$	Δ mass (ppm)
1.1	17.4	0.13	di-	*Z*-ε-viniferin (**1**)	$C_{28}H_{22}O_6$	454.1416	453.1337	453.1340	−0.7
1.2	17.9	2.80	di-	*E*-ε-viniferin (**2**)	$C_{28}H_{22}O_6$	454.1416	453.1337	453.1323	3.1
1.4	18.5	na	di-	*E*-ω-viniferin (**3**)	$C_{28}H_{22}O_6$	454.1416	453.1337	453.1340	−0.7
1.4	18.5	na	di-	*Z*-ω-viniferin (**4**)	$C_{28}H_{22}O_6$	454.1416	453.1337	453.1338	−0.2
2.1	13.5	1.10	di-	caffeic acid and catechin condensation product (**5**)	$C_{24}H_{20}O_9$	452.1107	451.1028	451.1021	1.6
2.2	14.8	1.39	di-	pallidol (**6**)	$C_{28}H_{22}O_6$	454.1416	453.1337	453.1317	4.4
3.1	15.4	0.61	tri-	ampelopsin D (**7**) + quadrangularin A (**8**)	$C_{28}H_{22}O_6$	454.1416	453.1337	453.1340	−0.7
3.2	18.9	1.13	tri-	α-viniferin (**9**)	$C_{42}H_{30}O_9$	678.1890	677.1811	677.1818	−1.0
4.1	19.1	0.59	tri-	*E-cis*-miyabenol C (**10**)	$C_{42}H_{32}O_9$	680.2046	679.1967	679.1979	−1.8
5.1	17.9	0.54	tri-	*Z*-miyabenol C (**11**)	$C_{42}H_{32}O_9$	680.2046	679.1967	679.1974	−1.0
5.2	18.1	1.55	tri-	*E*-miyabenol C (**12**)	$C_{42}H_{32}O_9$	680.2046	679.1967	679.1969	−0.3
6.1	16.8	5.46	tetra-	isohopeaphenol (**13**)	$C_{56}H_{42}O_{12}$	906.2676	905.2597	905.2617	−2.2
7.1	17.5	1.04	tetra-	ampelopsin H (**14**)	$C_{56}H_{42}O_{12}$	906.2676	905.2597	905.2620	−2.5
7.2	17.5	0.90	tetra-	vaticanol C-like (**15**)	$C_{56}H_{42}O_{12}$	906.2676	905.2597	905.2635	−4.2

mass analyzer. Electrospray mass spectra ranging from m/z 100 to 1500 were taken in positive mode with a dwell time of 0.1.

At the end of the 27 min run with mass spectra taken in positive mode, a 1 min run in negative mode was added. The cone voltage (CV) was set in scan mode at 40 V values for identification based on the aglycone peak and at 25 V for identification based on both the aglycone fragment and molecular ion. The following single ions (m/z) were monitored for quantification: 229.1 (CV = 25 V) for *trans*- and *cis*-resveratrol, 229.1 (CV = 40 V) for *trans*- and *cis*-piceid derivatives, 455.2 (CV = 60 V) for dimers, 681.2 (CV = 70 V) for trimers, and 907.2 (CV = 80 V) for tetramers.

Q-TOF Analysis. Accurate mass spectra were acquired using a Waters HDMS-Q-TOF Synapt mass spectrometer with an electrospray ionization system (ESI) and MassLynx 4.1 software (Waters Corp.). HDMS analysis was performed after separation in the chromatographic conditions described for the HPLC-DAD-MS analysis, in negative mode under the following conditions: capillary voltage, 2.5 kV; sampling cone, 25 V; extraction cone, 3 V; source temperature, 150 °C; desolvation temperature, 500 °C; cone gas flow (N_2), 50 L/h; desolvation gas flow (N_2), 1000 L/h. The m/z range was 50−3000 Da. The MS was calibrated using sodium formate, and leucine enkephalin was used as the lock mass. Experimental data are reported in Table 1. Under these conditions the instrument is expected to provide experimental data with an accuracy within ±3 ppm.

NMR Experiments. ^{1}H (400 MHz) and ^{13}C (100 MHz) NMR spectra for all of the isolated oligomers were recorded in d_6-acetone (99.90% CD_3COCD_3) at 298 K on a Bruker Avance 400 MHz NMR spectrometer, by using a 5 mm BBI probe with 90° proton pulse length of 8.7 μs at a transmission power of 0 db and equipped with pulsed-gradient field utility. The chemical shift scale (δ) was calibrated on the residual proton signal of deuterated acetone at δ_H 2.040 and δ_C 29.80. The following experiments were done: ^{1}H NMR; decoupled ^{13}C NMR; ^{1}H−^{1}H DQCOSY; ^{1}H−^{13}C HSQC; ^{1}H−^{13}C HMBC; and ^{1}H−^{1}H NOESY.

Molecular mechanics calculations were carried out by the computer program PCMOD 7.0/GMMX version 1.5 (Serena Software, Bloomington, IN). All of the minimized structures falling in a strain-energy window of 3.0 kcal/mol were saved and finally minimized with both MMX and MM3 force fields, keeping only those falling in a 2.0 kcal/mol.

UV Measurements. The UV spectra of all isolated oligomers were recorded in methanol, on a Hitachi U-2000 spectrometer (Tokyo, Japan). The average values were obtained by measuring two appropriate concentrations, one twice the other, all being in the range of $(1.15-9.55) \times 10^{-5}$ M, to obtain an absorbance value in the range of 0.27−0.83 UA.

Polarimetric and Circular Dichroic (DC) Measurements. The specific optical rotations were recorded in methanol at room temperature using a Jasco DP181 polarimeter at the sodium emission wavelength and evaluated as $[\alpha]_D$ values in deg dm^{-1} cm^3 g^{-1}. The CD spectra were recorded in methanol at room temperature using a Jasco J-40AS dichrograph and evaluated as $\Delta\varepsilon$ (molar circular dichroism) in cm mol^{-1} L at the maximum wavelength observed in the CD spectra.

STRUCTURAL DATA OF THE ISOLATED COMPOUNDS

According to current practice, we have consistently used only the *trans* and *cis* nomenclature to describe the stereochemistry at saturated rings, whereas the *Z*/*E* nomenclature has been used to describe the stereochemistry of double bonds. The names used in this study (together with the trivial names used in the literature) are as follows: *Z*-ε-viniferin (*cis*-ε-viniferin); *E*-ε-viniferin (*trans*-ε-viniferin); *E*-δ-viniferin (*trans*-δ-viniferin, *trans*-resveratrol dehydrodimer); *Z*-miyabenol C (*cis*-miyabenol C); *E*-miyabenol C (*trans*-miyabenol C).

***Z*-ε-Viniferin (1, Isolated in Fraction 1.1).** ESI-Q-TOF $(M-H)^-$ peak at m/z 453.1340; exact mass for $C_{28}H_{21}O_6$ 453.1344 (Table 1); $\Delta\varepsilon$ = −4.5 (301 nm), −2.9 (265 nm), +13.9 (233 nm), +29.8 (205 nm).

(+)-*E*-ε-Viniferin (2, Isolated in Fraction 1.2). ESI-Q-TOF $(M-H)^-$ peak at m/z 453.1323; exact mass for $C_{28}H_{21}O_6$ 453.1344 (Table 1); $\Delta\varepsilon$ = −7.6 (308 nm), +30.3 (236 nm); $[\alpha]_{589}$ (MeOH, *c* 0.32) = +34°.

ω-Viniferins (Isolated in Fraction 1.4). *E-ω-Viniferin (**3**).* ^{1}H NMR (analysis of 2:1 mxture of *E*/*Z* stereoisomers) δ 7.22 (d, *J* = 8.4 Hz, 2H, H2b+H6b), 7.03 (d, *J* = 8.6, 2H, H2a+H6a), 6.94 (d, *J* = 16.4 Hz, 1H, H7b), 6.76 (d, *J* = 16.4 Hz, 1H, H8b), 6.74 (d, *J* = 8.6 Hz, 2H, H3b+H5b), 6.72 (d, *J* = 2.1 Hz, 1H, H14b), 6.60 (d, *J* = 8.6 Hz, 2H, H3a+H5a), 6.32 (d, *J* = 2.1 Hz, 1H, H12b), 5.96 (t, *J* = 2.2 Hz, 1H, H12a), 5.86 (d, *J* = 8.0 Hz,

1H, H7a), 5.80 (d, J = 2.2 Hz, 2H, H10a+H14a), 4.70 (d, J = 8.0 Hz, 1H, H8a); ^{13}C NMR (from HSQC) δ 130.4 (C7b), 128.8 (C2b+C6b), 128.6 (C2a+C6a), 123.6 (C8b), 116.1 (C3a+C5a), 114.9 (C3b+C5b), 108.4 (C10a+C14a), 104.3 (C14b), 101.4 (C12a), 96.90 (C12b), 90.1 (C7a), 53.3 (C8a).

ESI-Q-TOF $(M - H)^-$ peak at m/z 453.1340; exact mass for $C_{28}H_{21}O_6$ 453.1344 (Table 1); $\Delta\varepsilon$ (from the 2:1 mixture 1.4E+1.4Z) = −9.2 (306 nm), +16.4 (231 nm).

*Z-ω-Viniferin (**4**).* ^{1}H NMR NMR (analysis of 2:1 mxture of E/Z stereoisomers) δ 7.04 (d, J = 8.4 Hz, 2H, H2b+H6b), 6.98 (d, J = 8.6 Hz, 2H, H2a+H6a), 6.72 (d, J = 2.1 Hz, 1H, H14b), 6.71 (d, J = 8.6 Hz, 2H, H3b+H5b), 6.59 (d, J = 8.6 Hz, 2H, H3a+H5a), 6.34 (d, J = 2.1 Hz, 1H, H12b), 6.32 (d, J = 12.0 Hz, 1H, H8b), 5.96 (t, J = 2.2 Hz, 1H, H12a), 6.01 (d, J = 12.1 Hz, 1H, H7b), 5.71 (d, J = 8.0 Hz, 1H, H7a), 5.69 (d, J = 2.2 Hz, 2H, H10a+H14a), 4.26 (d, J = 8.0 Hz, 1H, H8a); ^{13}C NMR (from HSQC) δ 131.2 (C7b), 130.4 (C2b+C6b), 128.8 (C2a+C6a), 125.8 (C8b), 115.8 (C3b+C5b), 114.9 (C3a+C5a), 108.5 (C10a+C14a), 104.3 (C14b), 101.4 (C12a), 96.8 (C12b), 90.2 (C7a), 52.7 (C8a).

ESI-Q-TOF $(M - H)^-$ peak at m/z 453.1338; exact mass for $C_{28}H_{21}O_6$ 453.1344 (Table 1); $\Delta\varepsilon$ (from the 2:1 mixture 1.4E+1.4Z) = −3.1 (270 nm), −2.6 (243 nm), +8.7 (225 nm).

Product of Condensation between Catechin and Caffeic Acid, 5 (Isolated in Fraction 2.1). ^{1}H NMR δ 6.89 (d, J = 2.1 Hz, 1H, H-2′), 6.80 (d, J = 8.1 Hz, 1H, H-5′), 6.75 (dd, J = 2.1, 8.1 Hz, 1H, H-6′), 6.71 (d, J = 8.1 Hz, 1H, H-5″), 6.64 (d, J = 1.9 Hz, 1H, H-2″), 6.53 (dd, J = 2.1, 8.1 Hz, 1H, H-6″), 6.24 (s, 1H, H6), 4.66 (d, J = 8.0 Hz, 1H, H-2), 4.49 (dd, J = 6.9, 2.0 Hz, 1H, H-β), 4.08 (ddd, J = 5.5, 7.1, 8.0 Hz, 1H, H-3), 3.07 (ddd, J = 6.9, 15.9 Hz, 1H, H-α_{ax}), 2.93 (dd, J = 5.5, 16.1 Hz, 1H, H-4$_{eq}$), 2.88 (dd, J = 2.0, 15.9 Hz, 1H, H-α_{eq}), 2.67 (dd, J = 7.9, 16.2 Hz, 1H, H-4$_{ax}$).

It contained a minimal amount (ca. 6%) of the diastereoisomer with opposite configuration at Cβ, having selected ^{1}H NMR signals of δ_H 5.00 (dd, J = 6.9, 8.4 Hz, 0.06H, H-β), 3.33 (dd, J = 8.4, 15.7 Hz, 0.06H, H-α_{eq}), 3.08 (dd, J = 6.9, 15.7 Hz, 0.06H, H-α_{ax}), 4.65 (d, J = 8.0 Hz, 0.06H, H-2), 4.08 (dd, J = 5.2, 7.8 Hz, 0.06H, H-3), 3.00 (dd, J = 5.2, 16.2 Hz, 0.06H, H-4$_{eq}$), 2.58 (dd, J = 7.8, 16.2 Hz, 0.06H, H-4$_{ax}$).

^{13}C NMR for the major stereoisomer: δ 167.9 (s, −COO−), 155.6 (s, C5), 154.1 (s, C7), 145.9 (s, C3″), 145.5 (s, C4″), 151.8 (s, C8a), 134.8 (s, C1″), 131.7 (s, C1′), 119.9 (d, C6′), 119.0 (d, C6″), 116.2 (d, C5″), 115.8 (d, C5′), 115.3 (d, C2′), 115.0 (d, C2″), 106.7 (s, C8), 101.8 (s, C4a), 99.4 (d, C6), 82.8 (d, C2), 67.7 (d, C3), 37.8 (t, Cα), 34.8 (d, Cβ), 28.4 (t, C4).

ESI-Q-TOF $(M - H)^-$ peak at m/z 451.1021; exact mass for $C_{24}H_{19}O_9$ 451.1035 (Table 1); $\Delta\varepsilon$ = −1.9 (289 nm), −2.2 (227 nm), +11.0 (214 nm).

Pallidol (6, Isolated in Fraction 2.2). ESI-Q-TOF $(M - H)^-$ peak at m/z 453.1317; exact mass for $C_{28}H_{21}O_6$ 453.1344 (Table 1); $\Delta\varepsilon$ = −10.3 (235 nm), +3.4 (218 nm); $[\alpha]_{589}$ (MeOH, c 0.02) ∼ 0°; $[\alpha]_{365}$ (MeOH, c 0.02) +47°.

Ampelopsin D (7) and Its Regioisomer, Quadrangularin A (8) (Isolated in Fraction 3.1b). ESI-Q-TOF $(M - H)^-$ peak at m/z 453.1340; exact mass for $C_{28}H_{21}O_6$ 453.1344 (Table 1).

α-Viniferin (9, Isolated in Fraction 3.2). ESI-Q-TOF $(M - H)^-$ peak at m/z 679.1818; exact mass for $C_{42}H_{29}O_9$ 679.1817 (Table 1); $\Delta\varepsilon$ = +5.4 (299 nm), +9.5 (249 nm), −10.1 (222 nm); $[\alpha]_{589}$ (MeOH, c 0.14) = −46°.

***E-cis*-Miyabenol C (10, Isolated in Fraction 4.1).** ^{1}H NMR δ 7.25 (d, J = 8.6 Hz, 2H, H2b+H6b), 7.05 (d, J = 8.6 Hz, 2H, H2c+H6c), 6.93 (d, J = 8.4 Hz, 2H, H2a+H6a), 6.92 (d, J = 16.4 Hz, 1H, H7c), 6.90 (d, J = 8.6 Hz, 2H, H3b+H5b), 6.77 (d, J = 8.6 Hz, 2H, H3c+H5c), 6.77 (d, J = 2.1 Hz, 1H, H14b+H14c), 6.60 (d, J = 8.6 Hz, 2H, H3a+H5a), 6.35 (d, J = 2.1 Hz, 1H, H12b), 6.25 (d, J = 16.4 Hz, 1H, H8c), 6.24 (d, J = 2.1 Hz, 1H, H12c), 5.98 (m, 2H, H12a+H14b), 5.67 (d, J = 2.1 Hz, 2H, H10a+H14a), 5.65 (d, J = 7.5 Hz, 1H, H7a), 5.22 (d, J = 6.8 Hz, 1H, H7b), 4.48 (d, J = 6.8 Hz, 1H, H8b), 3.71 (d, J = 7.5 Hz, 1H, H8a); ^{13}C NMR δ 162.8 (C11c), 162.0 (C11b), 159.5 (C13b+C13c), 158.7 (C11a+C13a), 158.2 (C4b+C4c), 157.7 (C4a), 142.2 (C9a), 141.1 (C9b), 136.0 (C1a), 133.2 (C1b), 130.1 (C7c), 128.80 (C2b+C6b+C2c+C6c), 128.5 (C2a+C6a), 122.7 (C10b), 117.5 (C10c), 116.3 (C3b+C6b+C3c+C5c), 115.6 (C3a+C5a), 108.2 (C10a+C14a+C14b), 103.7 (C14c), 101.7 (C12a), 96.8 (C12b+C12c), 93.3 (C7b), 90.2 (C7a), 53.9 (C8b), 52.7 (C8a).

ESI-Q-TOF $(M - H)^-$ peak at m/z 679.1979; exact mass for $C_{42}H_{31}O_9$ 679.1974 (Table 1); $\Delta\varepsilon$ = +3.7 (282 nm), +13.8 (237 nm), −12.8 (219 nm).

***Z*-Miyabenol C (11, Isolated in Fraction 5.1).** ^{1}H NMR δ 7.12 (d, J = 8.6 Hz, 2H, H2a+H6a), 6.84 (d, J = 8.6 Hz, 2H, H3a+H5a), 6.72 (d, J = 8.6 Hz, 2H, H2c+H6c), 6.55 (d, J = 8.6 Hz, 2H, H3b+H5b), 6.51 (d, J = 8.6 Hz, 2H, H3c+H5c), 6.38 (d, J = 8.4 Hz, 2H, H2b+H6b), 6.33 (d, J = 2.1 Hz, 1H, H12c), 6.26 (d, J = 2.1 Hz, 1H, H12b), 6.23 (t, J = 2.1 Hz, 1H, H12a), 6.12 (d, J = 2.1 Hz, 1H, H14c), 6.09 (d, J = 2.1 Hz, 1H, H14b), 5.93 (d, J = 2.1 Hz, 2H, H10a+H14a), 5.82 (d, J = 12.4 Hz, 1H, H8c), 5.78 (d, J = 12.4 Hz, 1H, H7c), 5.29 (d, J = 2.9 Hz, 1H, H7a), 5.26 (d, J = 2.6 Hz, 1H, H7b), 4.24 (d, J = 2.9 Hz, 1H, H8a), 3.86 (d, J = 2.6 Hz, 1H, H8b); ^{13}C NMR δ 161.8 (C11b+C11c), 159.4 (C13b+C13c), 158.7 (C11a+C13a), 158.4 (C4b), 158.0 (C4c), 157.0 (C4a), 147.8 (C9a), 143.2 (C9b+C9c), 136.8 (C1c), 134.7 (C1a), 133.2 (C1b), 131.2 (C7c), 130.7 (C2c+C6c), 127.2 (C2a+C6a), 125.3 (C8c), 126.6 (C2b+C6b), 121.7 (C10c), 119.4 (C10b), 115.5 (C3a+C5a+C3b+C5b+C3c+C5c), 108.1 (C14c), 106.8 (C14b), 106.5 (C10a+C14a), 102.1 (C12a), 96.5 (C12c), 95.8 (C12b), 93.5 (C7a), 92.1 (C7b), 56.6 (C8a), 52.5 (C8b).

ESI-Q-TOF $(M - H)^-$ peak at m/z 679.1969; exact mass for $C_{42}H_{31}O_9$ 679.1974 (Table 1); $\Delta\varepsilon$ = −1.9 (288 nm), −11.4 (250 nm), −38.6 (213 nm).

***E*-Miyabenol C (12, Isolated in Fraction 5.2).** ESI-Q-TOF $(M - H)^-$ peak at m/z 679.1969; exact mass for $C_{42}H_{31}O_9$ 679.1974 (Table 1).

Isohopeaphenol (13, Peak 6.1). ESI-Q-TOF $(M - H)^-$ peak at m/z 905.2617; exact mass for $C_{56}H_{41}O_{12}$ 905.2604 (Table 1); $\Delta\varepsilon$ = −8.2 (290 nm), +17.3 (242 nm), −73.0 (216 nm); $[\alpha]_{589}$ (MeOH, c 0.40) = −180°.

Ampelopsin H (14, Peak 7.1). ESI-Q-TOF $(M - H)^-$ peak at m/z 905.2620; exact mass for $C_{56}H_{41}0_{12}$ 905.2604 (Table 1); $\Delta\varepsilon$ = +24.6 (234 nm), −67.0 (218 nm), +126.8 (207 nm).

Vaticanol-C-like Isomer (15, Peak 7.2). ^{1}H NMR δ 7.60 (d, J = 8.6 Hz, 2H, H2a+H6a), 7.35 (d, J = 8.6 Hz, 2H, H2d+H6d), 7.06 (d, J = 8.6 Hz, 2H, H3d+H5d), 6.92 (br d, J = 8.6 Hz, 2H, H2c+H6c), 6.91 (d, J = 8.6 Hz, 2H, H3a+H5a), 6.55 (br d, J = 8.6 Hz, 2H, H3c+H5c), 6.29 (t, J = 2.1 Hz, 1H, H12a), 6.28 (s, 1H, H12c), 6.22 (s, 1H, H12b), 6.15 (d, J = 8.6 Hz, 2H, H2b+H6b), 6.05 (s, 1H, H12d), 6.00 (d, J = 2.1 Hz, 2H, H10a+H14a), 5.93 (d, J = 2.1 Hz, 2H, H10d+H14d), 5.93 (d, J = 11.1 Hz, 1H, H7a), 5.32 (d, J = 2.7 Hz, 1H, H7d), 5.18 (d, J = 11.1 Hz, 1H, H8a), 4.50 (d, J = 2.7 Hz, 1H, H8d), 4.32 (d, J = 11.1 Hz, 1H, H7c), 4.00 (d, J = 11.1 Hz, 1H, H8c), 4.00 (s, 1H, H7b), 3.78 (s, 1H, H8b); ^{13}C NMR δ 160.4, 158.7, 158.2, 156.8,

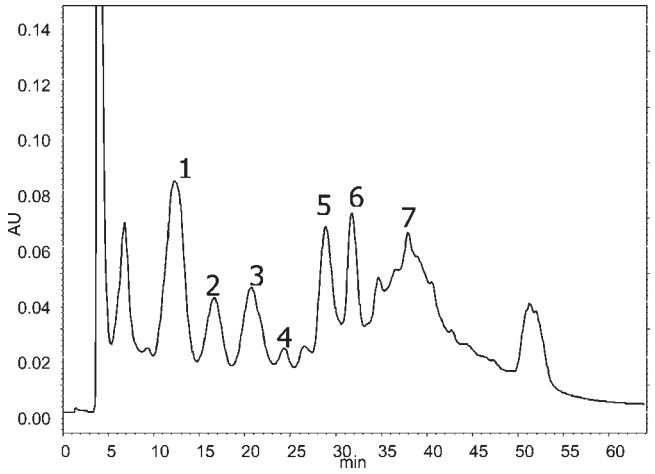

Figure 1. Purification through a diol column of the raw extract.

158.5, 155.1, 141.8, 140.8, 137.6, 134.5, 133.9, 130.4, 128.8, 128.6, 127.8, 118.3, 117.1, 116.4, 116.1, 115.0, 114.8, 109.7, 106.9, 106.2, 104.9, 103.5, 93.8, 90.2, 61.4, 56.6, 52.9, 48.5, 47.1, 45.2.

ESI-Q-TOF $(M - H)^-$ peak at m/z 905.2635; exact mass for $C_{56}H_{41}0_{12}$ 905.2604 (Table 1); $\Delta\varepsilon = -3.8$ (294 nm), +38.8 (238 nm), −32.3 (215 nm).

RESULTS AND DISCUSSION

Grape Infection, Extraction from Leaves, and Fractionation. In a preliminary survey using HPLC-DAD-MS, we observed that in leaves infected with *P. viticola* collected from the offspring of the Merzling × Teroldego cross, there was formation of many other stilbenes and stilbenoids, in addition to *trans*-resveratrol, *trans*-piceid, and *E*-ε-viniferin, in numbers exceeding those of known compounds isolated to date in grapes (unpublished results). Accurate identification and quantitation of minute amounts of viniferins in a complex matrix such as leaf extract is particularly demanding. At this point it was clear that before describing the interaction between the grapevine and *P. viticola* in this population, it was necessary to isolate and characterize these new metabolites. Eighteen high-stilbenoid producer genotypes were selected from the population, and these plants were infected and the apical leaves collected, pooled, and extracted with methanol, yielding enough material to perform isolation in sufficient amounts to elucidate the structure.

Prepurification of the extract took place in two steps. In agreement with previous results with stilbenoids from grape roots,[9,10] flash chromatography on a polystyrene−divinylbenzene resin (Isolute ENV+) made it possible to effectively eliminate most primary metabolites, such as carbohydrates, organic acids, amino acids, and chlorophylls, and secondary metabolites such as proanthocyanidins in the aqueous washing and pentane−dichloromethane and methanol fractions. This initial purification increased the signal of stilbenes and stilbenoids, previously overlapping and partly covered by other interferents, on the HPLC-DAD-MS chromatogram. A second flash chromatography on HW40S resin allowed further purification of the extract, collecting only those compounds eluting in the 40−90 min range. All of the target compounds were recovered in the purified extract obtained, now representing the main compounds in the HPLC-DAD-MS chromatogram.

The diol column allowed us to effectively fractionate the purified extract, obtaining seven fractions, which were separated on the basis of both their size and affinity (Figure 1). Characterization of the compounds showed the separation of dimers (fractions 1−3) from trimers (fractions 3−5) and tetramers (fractions 6 and 7).

Each of the seven fractions obtained using normal-phase chromatography was further separated using reversed-phase chromatography. This complementary technique allowed us to collect 14 fractions containing from 0.13 to 5.46 mg (Table 1) of the pure oligomer, for a total of 14.74 mg. These fractions were labeled with a sequential numerical code, the first number representing the elution order in the normal phase column (Figure 1) and the latter the elution order in reversed-phase separation (Figure 2).

Structural Elucidation of the Compounds Isolated. High-resolution mass spectrometry confirmation of the isolated oligomers was performed in negative mode with a high-resolution mass detector. A very good match to theoretical mass was found for the compounds isolated, below 3 ppm for all but three and below 5 ppm for all of the compounds (Table 1).

The observation of the UV spectrum gave us some preliminary information. The stilbenic chromophore is basically characterized by the presence of three bands, conventionally referred to as I, II, and III.[11] Band I is located between 308 and 336 nm, whereas band II is in the region of 281−313 nm. They show typically high molar extinction coefficients and are directly related to the presence of a conjugated *E*-double bond. Band III, located around 230 nm, is less strong and is basically linked to the presence of phenolic moieties. The presence of a *cis*-stilbenic chromophore gives rise to different spectra, with an absorption maximum (band II) of lower intensity and of shorter wavelength compared with the *trans*-isomer.[11]

Besides the molar extinction coefficients, we measured the ratio of absorbance A_{280}/A_{230}, which was suggested to be informative for assigning the structure.[12] The ratio A_{280}/A_{230} was found (Figure 3) to assume low values (between 0.22 and 0.28) for five stilbenoid oligomers. Intermediate values were found for the three oligostilbene trimers (0.37−0.38) and for all of the dimers (0.38−0.52), whereas the highest values are those of *trans*-resveratrol monomers (1.00−1.10).

Multiple NMR experiments were performed to clarify each structure; moreover, CD and α experimental values were acquired and are discussed subsequently for each compound when appropriate. The stilbenoid oligomers present three peculiar structural features, which must be clearly defined in order to define their structures: (1) the stereochemistry of exocyclic double bonds, (2) the regiochemical position of the 4-hydroxy- and 3,5-dihydroxyphenyl groups at C7/C8, and (3) the relative (absolute eventually) stereochemistry of the chiral centers C7 and C8. The first aim is trivial because the magnitude of the ^3J (H7,H8) is diagnostic of *Z* (11−13 Hz) or *E* (15−17 Hz) double-bond stereochemistry. On the other hand, the definition of the regiochemistry at the various C7/C8 centers needs HMBC experiments. Basically, examination of the 2D-HMBC resonances of H7 and H8 often allows definition of the main atoms' connectivity of the whole oligomers.

The third aim can be considered the most difficult one, due to the fact that in the five-membered rings small changes in the geometry may alter significantly the dihedral angle between H7/H8 coupled nuclei, resulting in large variations in the value of their coupling constant. Although in 2,3-benzodihydrofurans

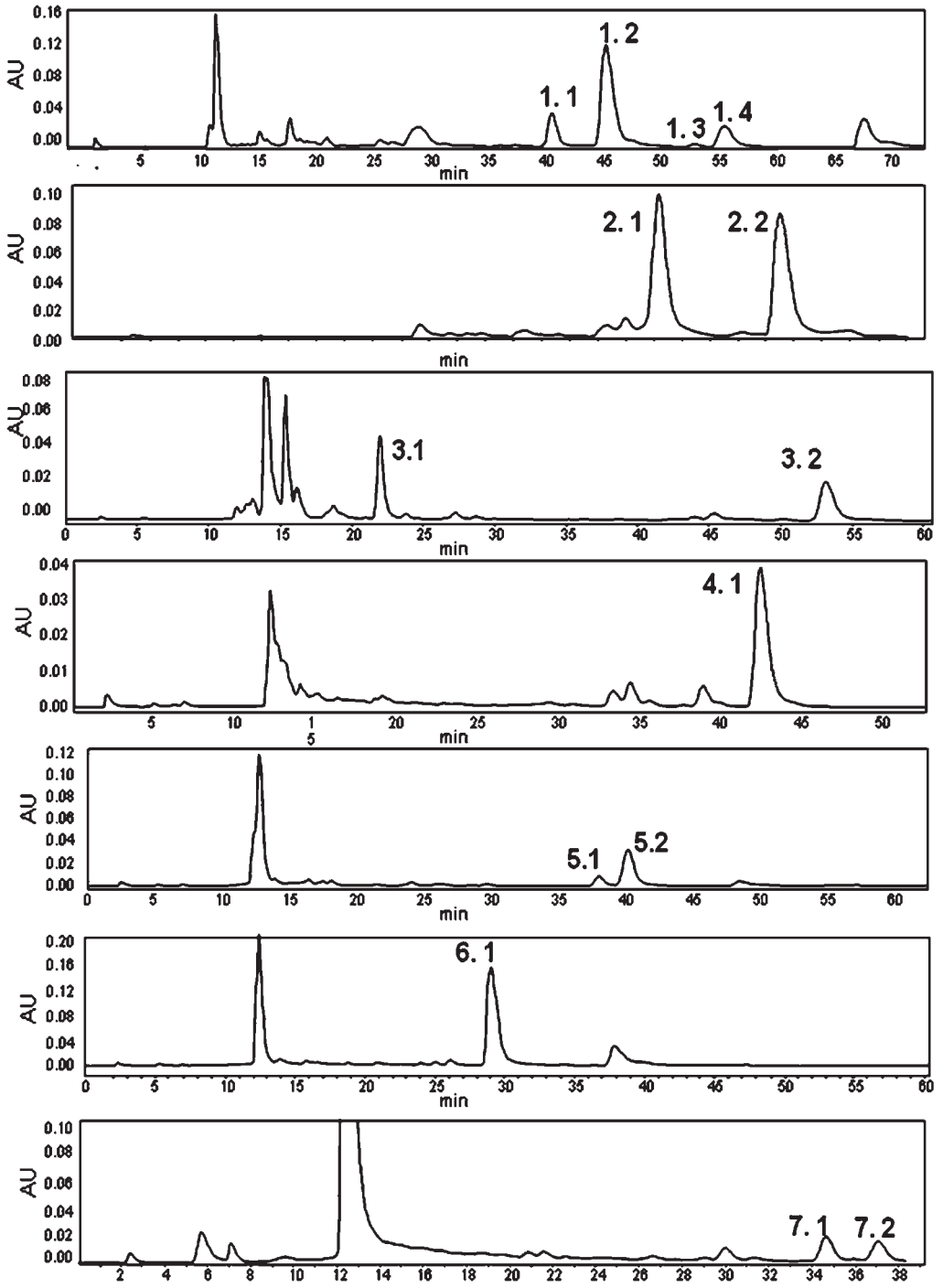

Figure 2. Final isolation by reversed-phase chromatography of the seven fractions obtained from the diol column.

(as well as in 2,3-dihydrofurans) it is generally accepted that $^{3}J_{cis}$ (5−10 Hz) is larger than $^{3}J_{trans}$ (1−9 Hz),[13] no firm assignment of stereochemistry can be made using the size of couplings alone, unless a specific substitution pattern or heterocyclic system has been carefully investigated or a full conformational analysis has been carried out. For example, in the case of benzodihydrofurans, changing the steric size of the substituents at positions 2 and 3 causes a reversal in the size of J_{cis} and J_{trans}. Therefore, this stereochemical assignment must be assessed by 2D-NOESY and/or NOE1D selective irradiation experiments. If by irradiation of H-7 resonance a marked NOE (≈10%) on the signal of the vicinal H-8 is observed, a spatial closeness of the involved protons is implied, and thus *cis* configuration at C7/C8 can be established, whereas if only a small NOE (≈1−2%) is detected, the two protons are expected to be in *trans* position. Eventually, the ^{13}C chemical shifts of C7 and C8 could discriminate between *cis* and *trans* 2,3 relative configuration due to the shielding effect of a *cis*-located carbon atom in γ-position (γ-effect).[14]

*Z-ε-Viniferin (**1**).* The MS of the peak isolated in fraction 1.1 (Figure 2) corresponded with that of a resveratrol dimer, with UV absorption and a molecular extinction coefficient ($\varepsilon_{280.0}$ = 9920 M^{-1} cm^{-1}) in agreement with the presence of one stilbenic

dx.doi.org/10.1021/jf200771y |*J. Agric. Food Chem.* 2011, 59, 5364–5375

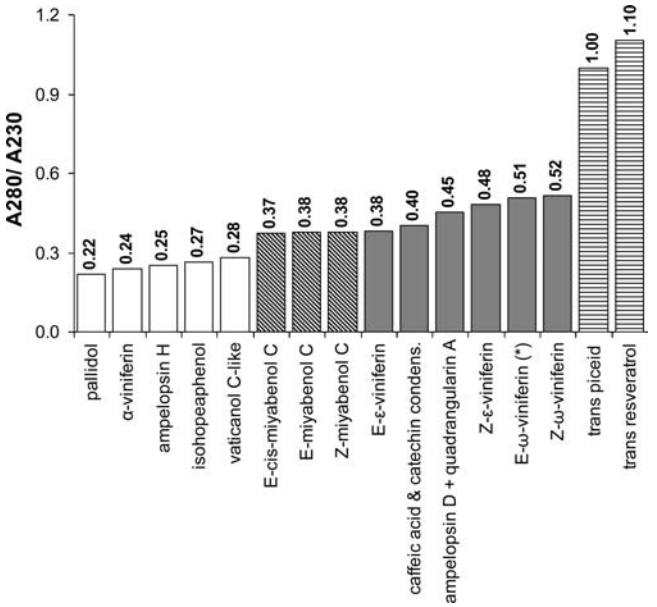

Figure 3. Absorbance ratio (A_{280}/A_{230}), that is, between UV bands II and III of the stilbenoids.

double bond in *cis*-configuration, and NMR (Figure 4) and CD data in agreement with the structure of *Z*-ε-viniferin. In particular, a complete assignment and a detailed discussion of NMR data for *Z*-ε-viniferin and all known compounds are reported in the Supporting Information

This compound was described as a product of light-induced isomerization of *E*-ε-viniferin extracted from vine leaves.[3] Because this compound was isolated in <5% of the *E*-isomer (Table 1) and was not observed in the analysis of fresh leaf extracts either, we believe that its presence was due to formation during isolation, even if the whole process was done with protection from light. It retained the same absolute configuration observed in the *E*-isomer (**2**).

*(+)-E-ε-Viniferin (**2**).* The MS of the peak isolated in fraction 1.2 (Figure 2) corresponded with that of a resveratrol dimer, with UV absorption and a molecular extinction coefficient ($\varepsilon_{319.0}$ = 30633 M^{-1} cm^{-1}; $\varepsilon_{280.0}$ = 24781 M^{-1} cm^{-1}) in agreement with the presence of one stilbenic double bond in *E*-configuration, and NMR (see the Supporting Information) (Figure 4), CD, and α data in agreement with the structure of (+)-*E*-ε-viniferin (**2**).

The isolation of only one specific dissymmetric *trans*-structure, the absolute configuration of which at the *trans*-dihydrobenzofuran ring was completely assigned and found to have both chiral centers in *S* configuration, confirmed the high specificity of the reaction of resveratrol dimerization, as already observed.[3]

The presence of this compound is very important, given the high bioactivity reported for *E*-ε-viniferin against the release of zoospores from the sporangia of *P. viticola* (50% inhibition at 19 μg/mL) and the motility of zoospores following their release (50% inhibition at 12.5 μg/mL), as well as in combating germination of the conidia of *Botrytis cinerea* (50% inhibition at 100 μg/mL). Moreover, *E*-ε-viniferin and *trans*-resveratrol are building blocks for many higher oligomers.

*ω-Viniferins (**3** and **4**).* The MS of the peak isolated in fraction 1.4 (Figure 2) corresponded with that of a mixture of two resveratrol dimers, with UV absorption maxima (294.5 nm) and an intermediate molecular extinction coefficient ($\varepsilon_{294.5}$ =

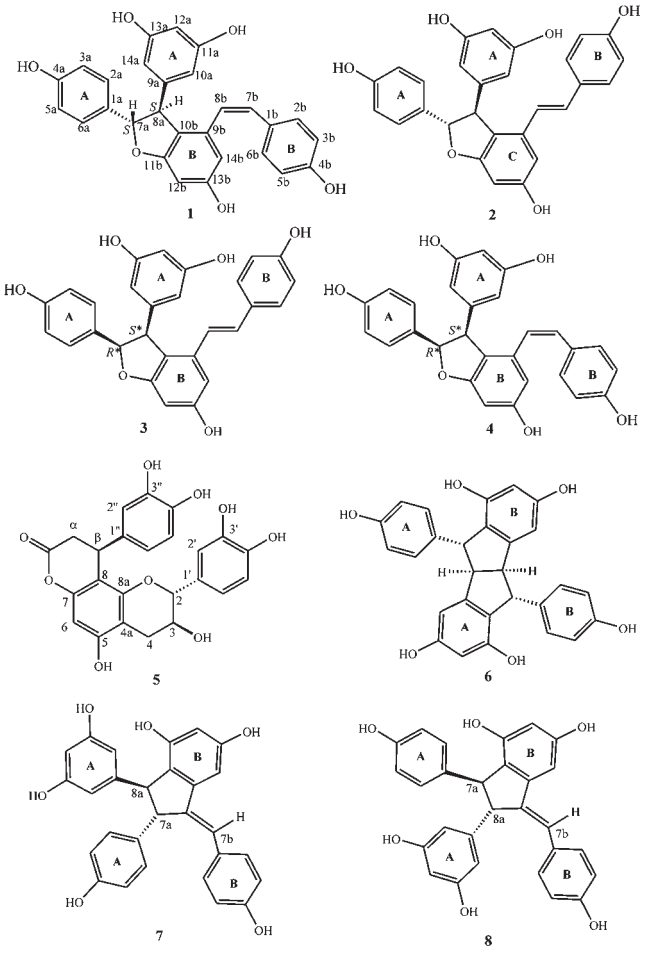

Figure 4. Structures of stilbenoid dimers in grapevine leaves (*Z*-ε-viniferin (**1**), *E*-ε-viniferin (**2**), *E*-ω-viniferin (**3**), *Z*-ω-viniferin (**4**), pallidol (**6**), *E*-ampelopsin D (**7**), *E*-quadrangularin A (**8**)) and of a condensation product between (+)-catechin and *trans*-caffeic acid (**5**).

13947 M^{-1} cm^{-1}), in agreement with the presence of a mixture of stilbenes with the double bond in *Z*+*E*-configuration. NMR (Figure 4) and CD data were in agreement with the presence of a mixture of two new isomers of ε-viniferin, which we named ω-viniferins (Figure 4). They were minor viniferins, because the amount collected was about 6.5 times less than that of the main dimer in the grape, *E*-ε-viniferin (**2**).

NMR and MS data pointed out that these resveratrol dimers were structural isomers of *E*- and *Z*-ε-viniferins. Because no changes in atom connectivity and/or the regiochemical position of aromatic moieties were found from HMBC-NMR measurements, the observed differences in NMR data must be due to a different stereochemical relationship at the chiral centers C7a and C8a. NOESY measurements allowed us to establish that in ω-viniferins H7a and H8a were not stereochemically *trans* related as usually found in resveratrol oligomers. In fact, for both the double isomers of ω-viniferins the integration of 2D-NOESY off-diagonal maps of H-7a showed a stronger dipolar effect with H-8a than with H2a/H6a, whereas the NOE effect of H7a with H10a/H14 was not detectable at all. This outcome, pointing to a 7,8 *cis* stereochemistry, is in perfect agreement with the internuclear distances evaluated in the molecular geometry of these compounds as obtained by MM calculations of both the ω-viniferins, whereby the H7a−H8a distance (2.34 Å) was found

dx.doi.org/10.1021/jf200771y |*J. Agric. Food Chem.* 2011, 59, 5364–5375

to be shorter than the H7a−H2a/H6a (2.68 Å), whereas the distance H7a−H10a/H14a was evaluated to be so long (4.19 Å) as to escape NOE detection. The value of the ^3J (H-7/H-8) coupling constant (8.0 Hz) is higher than in ε-viniferins, giving further support to their *cis* relationship.

Due to the intrinsically high capacity of the NMR technique for quantitative analysis, straighforward ^{1}H NMR measurements make it possible to obtain a reliable estimation of their relative molar ratio in the mixture. According to integration of the relative area of proton NMR signals for *E*-ω-viniferin (**3**) as compared to *Z*-ω-viniferin (**4**) signals, the relative abundance of the former must be 66% and the latter 33%. This was confirmed by successive fractionation of the two isomers, which allowed us to obtain their UV data: *E*-ω-viniferin (**3**), $\varepsilon_{318.5}$ = 19966 M^{-1} cm^{-1} and $\varepsilon_{280.0}$ = 12554 M^{-1} cm^{-1}; *Z*-ω-viniferin (**4**), $\varepsilon_{281.5}$ = 6754 M^{-1} cm^{-1}).

*Product of Condensation between (+)-Catechin and trans-Caffeic Acid (**5**).* The MS of the peak isolated in fraction 2.1 (Figure 2) suggested a highly oxygenated structure (Table 1) with a weaker UV chromophore with a maximum of 280.5 nm ($\varepsilon_{280.5}$ = 7344 M^{-1} cm^{-1}) and NMR and CD data in agreement with a product of condensation between (+)-catechin and *trans*-caffeic acid (Figure 4). The occurrence of the catechin skeleton could be deduced from the characteristic signals for H2 at 4.41 (d, J = 8.4 Hz). ^1J heterocorrelated to C2 (δ_C 82.8), which allowed us to establish the relevant C2−C3 stereochemistry. In fact, a very small coupling J(2,3 < 1 Hz) would be expected for H2 in epicatechin. The configuration at Cβ was determined by the coupling pattern of Hβ with the diastereotopic protons at Cα, although fast flipping of the lactone ring leads to averaged J values. Small signals detectable in the ^{1}H NMR and DQCOSY spectra of this sample indicated the presence of another compound, which could be assigned as its Cβ stereoisomer on the basis of significant changes in the chemical shifts of 2Hα and Hβ, whereas signals of the catechin moiety of both the stereoisomers were almost superimposable. Such a structure can be formed by C−C oxidative coupling of the carbon β to the carbonyl of caffeic acid with the C8 of catechin, which is then converted into the corresponding δ-lactone.

Isolation and characterization of this condensation product provided evidence that other major grapevine phenolics also participate in the enzymatic oxidative mechanisms induced by grapevine−pathogen interactions. This provided independent confirmation of the involvement of constitutive phenolics in grapevine resistance, in agreement with the known correlation between flavonoid content and the increased resistance of sun-exposed vine leaves to *P. viticola*.[15] A number of phenols and catechols have indeed been shown to act as a strong inhibitor of *B. cinerea* laccases. By inhibiting stilbene oxidase, the constitutive phenolics may attenuate the defense against *Botrytis*, leaving "safer ground" for the classical phythoalexins.[16]

*Pallidol (**6**).* The MS of the peak isolated in fraction 2.2 (Figure 2) corresponded with that of a resveratrol dimer. NMR (see the Supporting Information), CD, and α data were in agreement with the known strucure of pallidol (Figure 4).[17−19]

This stilbenoid is known to be easily produced from *trans*-resveratrol treated with *B. cinerea* cultures[20] or with peroxidases.[21] In the latter case, it was reported to yield (±)-pallidol. The lack of optical activity may be due not to racemization of its chiral centers but to the intrinsically low dissymmetry of the whole molecule, which contains an internal C2 axis of symmetry. Although, in principle, the presence of this element of symmetry does not make pallidol an achiral molecule, it could act to decrease its chiroptical properties. It is worthy of mention that the NMR data of "compound **4**" reported in Kulesh et al.[22] as optically active (−)-pallidol do not agree with true pallidol NMR data and are clearly inconsistent with any reasonable resveratrol dimer structure.

*Ampelopsin D (**7**) and Its Regioisomer, Quadrangularin A (**8**).* The MS of the peak isolated in fraction 3.1 (Figure 2) corresponded with that of a resveratrol dimer, with UV absorption and a molecular extinction coefficient ($\varepsilon_{313.5}$ = 24573 M^{-1} cm^{-1}, $\varepsilon_{280.0}$ = 15261 M^{-1} cm^{-1}) in agreement with the presence of one stilbenic double bond in *E*-configuration absorbing at 313.5 nm and NMR spectra in agreement with the presence of a mixture 1:1 of two compounds already identified as constitutive stilbenes in some Vitaceae, respectively, ampelopsin D (**7**)[23,24] and its regioisomer, quadrangularin A (**8**)[25] (Figure 4). Attribution of the structure to these *trans*-isomers required some attention and comparison with another similar structure, parthenocissin A[26] (see the Supporting Information for a detailed discussion of their NMR spectra) in light of the conflicting information discussed in the references cited.

Contrary to a literature report[25] claiming that "NMR data of ampelopsin D[23] are quite similar to those of quadrangularin A and its structure should be actually the same as that of quadrangularin A itself", we confirm here that a careful analysis of NMR data of our sample containing both dimers in almost equimolar amount leads definitively to the demonstration that these structures are different, in agreement with the spectroscopic reinvestigation by Niwa et al.[27]

It has been suggested[24] that (−)-ampelopsin D (**7**) is synthesized in the Vitaceae from its precursor (+)-*E*-ε-viniferin (**2**), via initial acid protonation of the oxygen atom on the dihydrofuran ring, followed by nucleophilic attack of the double bond and formation of a five-membered ring intermediate, which deprotonates to yield (−)-ampelopsin D (**7**). Such a mechanism, which could justify the presence of this compound, is incompatible with the formation of quadrangularin A.[24,27] A stereoselective reaction, following apparently a biomimetic cyclization of naturally occurring stilbenes during oxidative oligomerization, was shown to produce either ampelopsin D or quadrangularin A, via different mechanisms.[28] The presence of both ampelopsin D (**7**) and quadrangularin A (**8**) in hybrids of *V. vinifera* is thus reported here for the first time.

*α-Viniferin (**9**).* The MS of the peak isolated in fraction 3.2 (Figure 2) corresponded with that of a resveratrol trimer, with a medium-intensity UV choromophore ($\varepsilon_{282.5}$ = 6265 M^{-1} cm^{-1}) and A_{280}/A_{230} = 0.238 (Figure 3), in agreement with the presence of isolated phenols.

NMR (see the Supporting Information), UV, and CD data were in agreement with the known structure of α-viniferin (Figure 5), which was the first stilbenoid with antifungal properties discovered in vine leaves infected with *B. cinerea*.[29] This compound was also observed in vine leaves infected with *P. viticola*, but not in UV-irradiated leaves.[30]

In our case, amounts of the compound isolated were sufficient to provide its ^{13}C NMR and optical rotatory power for the first time, confirming a dissymmetric structure with $[\alpha]_{589}$ (MeOH, *c* 0.14) = −46°.

According to Langcake and Pryce,[3] α-viniferin inhibits the release of zoospores from the sporangia of *P. viticola* as well as the motility of the zoospores after their release and is also most active

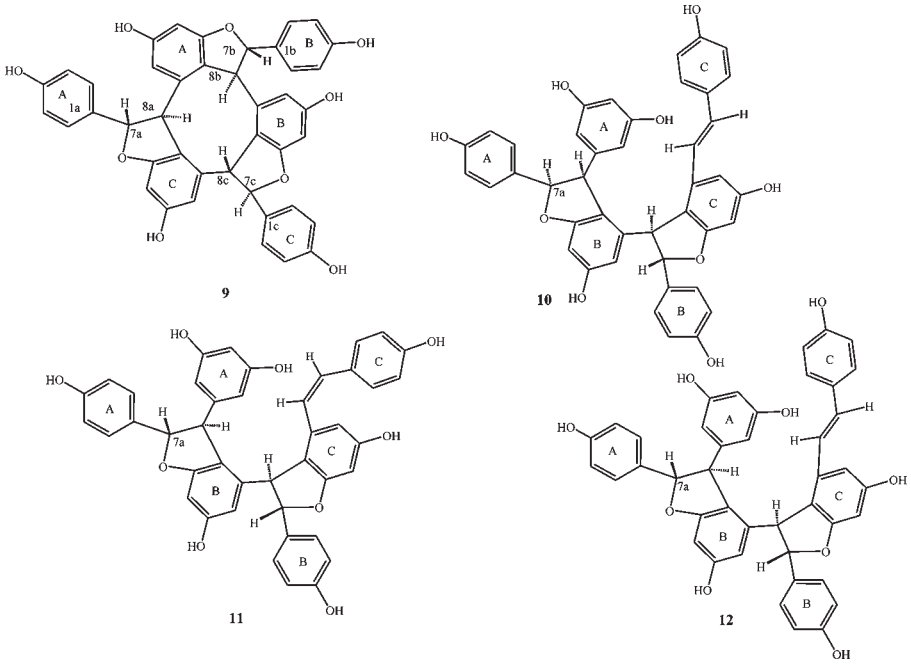

Figure 5. Structures of stilbenoid trimers in grapevine leaves: α-viniferin (**9**), *E-cis*-miyabenol C (**10**), *E*-miyabenol C (**12**), and *Z*-miyabenol C (**11**).

against germination of the conidia of *B. cinerea*. After the pioneering studies of Pryce and Langcake,[29] the presence of this compound, as well as other uncharacterized viniferin-like compounds, such as β-viniferin and γ-viniferin,[3] was neglected, possibly due to difficulties in relation to identification and characterization. As a consequence, our study is the first report confirming the presence of α-viniferin (**9**) in vine leaves infected with *P. viticola*.

*E-cis-Miyabenol C (**10**).* The molecular structures **10**, **11**, and **12** were closely correlated. The MS of **10**, isolated in fraction 4.1 (Figure 2), corresponded with that of a resveratrol trimer, with a strong UV choromophore ($\varepsilon_{320.5}$ = 11096 M^{-1} cm^{-1}, $\varepsilon_{280.0}$ = 8935 M^{-1} cm^{-1}) in agreement with the presence of one *trans*-stilbenic double bond in the structure. Both NMR and CD data were in agreement with a new stereoisomer of *E*-miyabenol C (Figure 5).

A careful NMR analysis of the HMBC traces suggested the same atom connectivity of *E*-miyabenol C (**12**), but NOESY measurements indicated a very strong dipolar NOE effects of the doublet δ_H 3.71 (H8a) with its vicinal proton H7a at δ_H 5.66 and a medium NOE with H8b. Thus, we obtained evidence to propose here the 7a,8a *cis*-stereochemistry for compound **10**. Strong differences in ^{13}C and ^{1}H NMR frequencies for almost all nuclei in the left side of the molecule (containing the *cis* ring junction) and strong δ similarities for those embedded in the opposite side support our assignment. MM calculations are also in agreement, pointing out a geometry optimized structure wherein the H7a−H7b and H8a,H8b torsional angles are found to be −24° and 149°, respectively, leading to evaluated J(7a,8a) = 6.8 Hz and J(7b,8b) = 8.9 Hz, in good agreement with their experimental values.

This new stereoisomer of miyabenol C may derive from the addition of a single oxidized *trans*-resveratrol intermediate, with the radical in the α position, on the stilbenic double bond, to the *m*-diphenol ring of the dimer (+)-*E*-ε-viniferin. The stereochemistry of (+)-*E*-ε-viniferin is completely retained, whereas the newly formed dihydrofuran ring has the same uncommon *cis*-stereochemistry already found in ω-viniferins (**3**,**4**). Similar stereochemistry in the condensation of the terminal resveratrol unit has already been observed in the formation of the tetramer kobophenol A from *E*-miyabenol C in the roots of *Carex kobomugi* Ohwi.[31]

*Z-Miyabenol C (**11**).* The MS of the peak isolated in fraction 5.1 (Figure 2) corresponded with that of a resveratrol trimer, with a strong UV choromophore ($\varepsilon_{281.5}$ = 14025 M^{-1} cm^{-1}), in agreement with the presence of one *cis*-stilbenic double bond in the structure. Both NMR and CD data were in agreement with the structure of *Z*-miyabenol C (**11**) (Figure 5),[31] which had not previously been reported in the grapevine.

NMR data for this compound are almost superimposable to those of miyabenol C in the A and B moieties, whereas significant differences are present in the neighboring of C moiety due to the presence of a *Z* 7c/8c double bond. The relative stereochemistry at 7a/8a and at 7b/8b chiral centers was established to be *trans* according to NOE effects of the corresponding proton signals. Moreover, the strong NOE observed between H8a and H8b in the NOESY spectrum suggested a *cisoid* relationship in this structure.

*E-Miyabenol C (**12**).* The MS of the peak isolated in fraction 5.2 (Figure 2) corresponded with that of a resveratrol trimer, and both NMR and CD data were in agreement with the structure of *E*-miyabenol C (**12**, Figure 5). It was not possible to measure its UV molar extinction coefficient with precision, because this compound partially rearranged in solution, yielding a mixture of the *cis*- and *trans*-isomers. However, our NMR and CD data agreed well with the literature.[31,32] In particular, the benzodihydrofuran streochemistry at C7a/C8a and C8a/8b has been confirmed to be *trans* and, as observed in **11**, a *cisoid* relationship of H8a with respect to H8b was found. The amount of **12** recovered from our vine leaves was the third highest of all the viniferins, and it was the main trimer (Table 1). This is in good agreement with the observation that its formation requires the

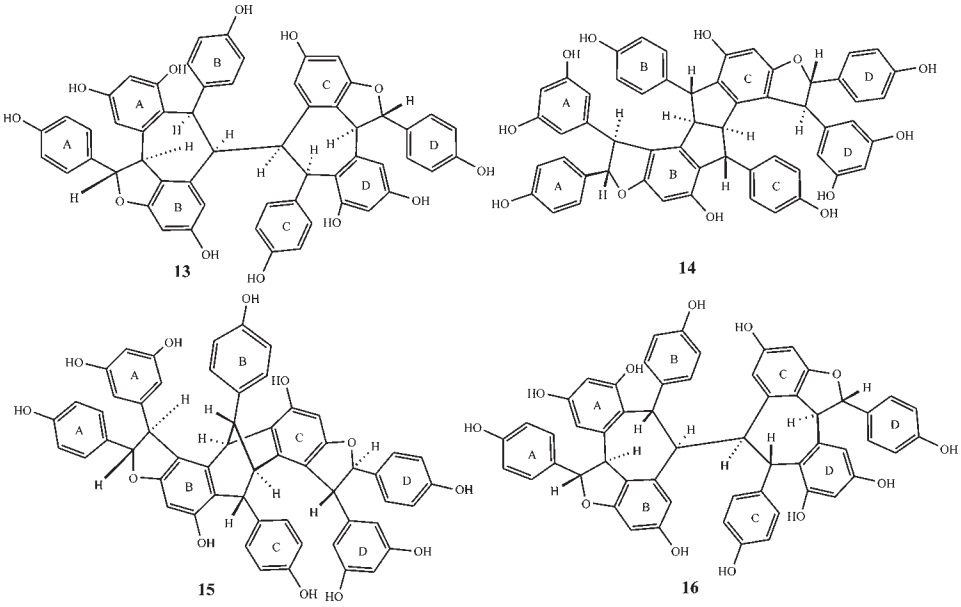

Figure 6. Structures of stilbenoid tetramers isolated from grapevine leaves: isohopeaphenol (**13**), ampelopsin H (**14**), vaticanol C isomer (**15**), and hopeaphenol (**16**).

addition of one resveratrol radical to **2**, which is the main dimer, repeating the same mechanism leading to the formation of **2** to obtain the sterochemistry of **12**.

E-Miyabenol C is reported here for the first time in vine leaves. Grapes are capable of synthesizing it, as it has already been isolated as a constitutive trimer in *V. vinifera* stalks.[33]

*Isohopeaphenol (**13**).* The MS of the peak isolated in fraction 6.1 (Figure 2) corresponded with that of a resveratrol tetramer, with a medium-intensity UV choromophore ($\varepsilon_{281.0}$ = 10929 M^{-1} cm^{-1}) and A_{280}/A_{230} = 0.266 (Figure 3), in agreement with the absence of conjugation between phenolic rings. NMR data (see the Supporting Information), CD, and α data were compatible with the known structure of the symmetric tetramer isohopeaphenol (**13**, Figure 6), a known viniferin already characterized in the cork of *V. vinifera* 'Kyohou'.[34]

The structure of isohopeaphenol was elucidated by comparing its NMR data with those of hopeaphenol **16** (Figure 6) (see the Supporting Information for a correct resonance assignment). Our NMR data are in good agreement with those of Ito et al.[34] for isohopeaphenol, although they did not report the NMR solvent used. The relative stereochemistry at the chiral centers has been confirmed by NOESY experiments.

Isohopeaphenol was observed here for the first time, the compound being isolated in by far the highest amounts in *P. viticola* infected vine leaves (Table 1). Hopeaphenol, a structurally very similar isomer, has already been isolated as a constitutive stilbenoid in the roots of *V. vinifera* cv. Chardonnay, where its concentration was in the range of 0.5−8 mg/g of fresh root.[9]

*Ampelopsin H (**14**).* The MS of the peak isolated in fraction 7.1 (Figure 2) corresponded with that of a resveratrol tetramer, with a medium-intensity UV choromophore ($\varepsilon_{281.0}$ = 12710 M^{-1} cm^{-1}) and A_{280}/A_{230} = 0.253 (Figure 3), in agreement with the absence of conjugation between phenolic rings. Both NMR and CD data (see the Supporting Information) were in agreement with the presence of a symmetric tetramer, with the structure of a pallidol derivative, corresponding with that of ampelopsin H (**14**, Figure 6).[23] This structure had not previously been found in grapes.

Ampelopsin H is a symmetric tetramer with a C2 axis leading to the chemical equivalence of hydrogen and carbon atoms in moieties A and B to those of moieties D and C, respectively. As a striking difference with pallidol, ampelopsin H shows strong Cotton effects in its CD spectrum, indicating that this compound should be enantiomerically pure. Moieties A and D with the same relative and absolute configurations at chiral centers 7a,8a and 7d, 8d linked to the internal ring system of pallidol (moieties B and C) seem to strengthen the overall dissymmetry of this molecule.

This tetramer may derive from the addition of two oxidized *trans*-resveratrol intermediates, both with the radical in the α position, on the stilbenic double bond, to each of the *m*-diphenol rings of the dimer pallidol (2.2). The stereochemistry of pallidol is completely retained at the center of the tetramer (Figure 6), whereas both newly formed dihydrofuran rings have *trans*-stereochemistry, according to NOESY measurements

*Vaticanol-C Isomer (**15**).* The MS of the peak isolated in fraction 7.2 (Figure 2) corresponded with that of a resveratrol tetramer, with a medium-intensity UV choromophore ($\varepsilon_{281,0}$ = 14832 M^{-1} cm^{-1}) and A_{280}/A_{230} = 0.280 (Figure 3), in agreement with the absence of conjugation between phenolic rings. NMR, CD, and optical rotation data were in agreement with the presence of an asymmetric tetramer, with a characteristic dibenzobicyclo[3.2.1]octadiene system, containing two dihydrofuran rings with their phenolic constituents in *trans*- configuration (Figure 6). Whereas NMR data for the partial moieties A and D are easily assigned by 2D-NMR techniques, the interpretation of the same data was much more complex when looking at the central part (moieties B and C) of this compound. The analysis was hindered not only by the low amount of this tetramer but, mainly, by the presence of several exchange-broadened peaks in its ^{1}H spectrum and by the low signal/noise ratio in HSQC and HMBC spectra. In particular, the ortho-coupled proton signals at H2c/H6c (6.92 ppm) and H3b/H5b (6.55 ppm) appear as very broad doublets, thus indicating a hindered rotation around the C1c−C7c single bond. Because four methine hydrogen atoms can be assigned by their characteristic H/C resonance to the

benzylic positions 7b/8b and 7c/8c, we assume that the structure of this tetramer should be an isomer of vaticanol C, but more detailed NMR investigations carried out in a higher amount of pure **15** are necessary to define its structure.

Vaticanol C has never been previously reported in *Vitis*, whereas it has already been isolated in the stem bark of *Vatica rassak* (Dipterocarpaceae)[35] during the search for stilbenoids with anticancer and hepatoprotective properties. It was recently found to be a strong inhibitor of matrix metalloproteinases (MMPs).[36] The particular structure of this vaticanol C isomer may possibly derive from direct condensation of two *E*-ε-viniferins, which condensate through their stilbenic double bonds, producing a dibenzobicyclo octadiene system. This would be consistent with the fact that NMR data are compatible with the hypothesis that they retained their configuration of **2** at both dihydrofuran rings.

In conclusion, three tetramers were isolated for the first time from *P. viticola* infected grapevine leaves. It is likely that one of these corresponds with the uncharacterized viniferin observed by Langcake and Pryce.[3] The amounts were quite high, comparable with that of *E*-ε-viniferin (Table 1).

Viniferin Formation Mechanism. The enzymes involved in the formation of viniferins are expressed both in pathogens and in plants. Evidence for the ability of grapevine to directly synthesize viniferins comes from their constitutive presence in large amounts in some parts of the plant, as a diversity of stilbenes[10,37] and stilbenoid oligomers,[9] which are present at gram per kilogram levels in vine roots. ε-Viniferin has also been reported to be a constitutive stilbene of grapevine clusters stems.[38] Moreover, synthesis of three dimers (two δ-viniferin glucosides and pallidol) has been demonstrated in *V. vinifera* cv. Gamay Freaux var. Tenturier cell cultures.[39]

"Inducible" viniferins can arise from the oligomerization of *trans*-resveratrol in grape tissues as an active defense strategy by the plant. They are hardly detectable in healthy leaves, and a number of reports proved the induction of a substantial accumulation of these compounds in infected leaves.

"Metabolized" viniferins could be produced or modified by exocellular enzymes released from the pathogen in an attempt to eliminate undesirable toxic compounds.

The pattern of viniferins found in infected leaves lacked some of the constitutive viniferins to date elucidated in healthy grape tissues, such as ampelopsin A and hopeaphenol,[9] r-viniferin,[37] r-2-viniferin,[10] gnetin H,[37] *trans*-miyabenol C,[33] *trans*-amurensin B, amurensin G, and ampelopsin F.[45] Whereas the presence of many optically active viniferins, rather than racemates, in our partially resistant genotypes suggested a high level of control of the biosynthesis, supporting the theory of "inducible" viniferins, it was not possible to rule out the possible presence of metabolites driven by fungal laccases and peroxidases. We did not observe the presence of δ-viniferin or any other stilbenoid formed through the involvement of a (C) resveratrol radical.[21]

The difference in the pattern of viniferins in our results and those obtained in previous studies[40−44] could be due to differences in the grape varieties or methods used and is compatible with the hypothesis that the plant, rather than the pathogen, is responsible for the complex pattern of viniferins observed in *P. viticola* infected leaves. In perspective, to assess whether the outcome of this study holds in general, it will be very interesting to investigate other resistant varieties challenged with different pathogens and analyze the viniferin accumulation profile.

The infected leaves accumulated a substantial amount of viniferins. It should be highlighted that stilbenoids, a class of "orphan" viniferins often neglected in previous studies, were by far the most important class in our Merzling × Teroldego genotypes from a quantitative point of view (Table 1).

Despite the unavoidable losses taking place in a complex isolation process, we recovered a total of 14.74 mg of viniferins (stilbenes and stilbenoids) from 517 g of leaves, namely, 28.5 mg/kg of FW. Such an amount is considered to be important for explaining the resistance of the plant, given the low concentration (usually in the μg/mL range) required for bioactivity against *P. viticola*. Moreover, the fact that these values were obtained from processing whole leaves should be taken into account, as it is known that they are absent in healthy leaves, because their presence is limited to the infected zone and a narrow surrounding fluorescent zone.[2] Further work is necessary to evaluate the bioactivity of the new oligomers, as in the case of isohopeaphenol, *E*-miyabenol C, vaticanol C isomer, and pallidol, as major stress metabolites accumulating in infected leaves of partially resistant Merzling × Teroldego genotypes.

■ ASSOCIATED CONTENT

Supporting Information. Scheme of the experiment and additional structural data of the isolated compounds. This material is available free of charge via the Internet at http://pubs.acs.org.

■ AUTHOR INFORMATION

Corresponding Author

*Phone: +39-0461-615259. Fax: +39-0461-615200. E-mail: fulvio.mattivi@iasma.it.

Funding Sources

This work was supported by the Project "Resveratrol" and ADP 2010, both funded by the Autonomous Province of Trento, Italy.

■ ACKNOWLEDGMENT

We thank Francesco Berghi for his assistance in setting up the preparative HPLC methods.

■ REFERENCES

(1) Bavaresco, L.; Fregoni, C.; Van Zeller de Macedo Basto Goncalves, M. I.; Vezzulli, S. Physiology and molecular biology of grapevine stilbenes: an update. In *Grapevine Molecular Physiology and Biotechnology*, 2nd ed.; Roubelakis-Angelakis, K. A., Ed.; Springer Science+Business Media: London, U.K., 2009; pp 341−364.

(2) Langcake, P.; Cornford, C. A.; Pryce, R. J. Identification of pterostilbene as a phytoalexin from *Vitis vinifera* leaves. *Phytochemistry* **1979**, *18*, 1025–1027.

(3) Langcake, P.; Pryce, R. J. A new class of phytoalexins from grapevines. *Experientia* **1977**, *33*, 151–152.

(4) Jeandet, P.; Douillet-Breuil, A. C.; Bessis, R.; Debord, S.; Sbaghi, M.; Adrian, M. Phytoalexins from the Vitaceae: biosynthesis, phytoalexin gene expression in transgenic plants, antifungal activity, and metabolism. *J. Agric. Food Chem.* **2002**, *50*, 2731–2741.

(5) Pezet, R.; Perret, C.; Jean-Denis, J. B.; Tabacchi, R.; Gindro, K.; Viret, O. δ-Viniferin, a resveratrol dehydrodimer: one of the major stilbenes synthesized by stressed grapevine leaves. *J. Agric. Food Chem.* **2003**, *51*, 5488–5492.

(6) Chong, J.; Poutaraud, A.; Hugueney, P. Metabolism and roles of stilbenes in plants. *Plant Sci.* **2009**, *177*, 143–155.

(7) Dell'Agli, M.; Galli, G. V.; Vrhovsek, U.; Mattivi, F.; Bosisio, E. In vitro inhibition of human cGMP-specific phosphodiesterase-5 by polyphenols from red grapes. *J. Agric. Food Chem.* **2005**, *53*, 1960–1965.

(8) Mattivi, F.; Reniero, F.; Korhammer, S. Isolation, characterization, and evolution in red wine vinification of resveratrol monomers. *J. Agric. Food Chem.* **1995**, *43*, 1820–1823.

(9) Reniero, F.; Rudolph, M.; Angioni, A.; Bernreuther, A.; Cabras, P.; Mattivi, F. Identification of two stilbenoids from *Vitis* roots. *Vitis* **1996**, *35*, 125–127.

(10) Korhammer, S.; Reniero, F.; Mattivi, F. An oligostilbene from *Vitis* roots. *Phytochemistry* **1995**, *38*, 1501–1504.

(11) Hillis, W. E.; Ishikura, N. The chromatographic and spectral properties of stilbene derivatives. *J. Chromatogr.* **1968**, *32*, 323–336.

(12) Mattivi, F.; Reniero, F. Relationship between UV spectra and molecular structure of resveratrol oligomers. *Polyphenols Commun.* **1996**, *96*, 125–126.

(13) Stevens, J. D.; Fletcher, H. G. Proton magnetic resonance spectra of pentofuranose derivatives. *J. Org. Chem.* **1968**, *33*, 1799–1805.

(14) Wehrli, F. W.; Wirtlin, T. In *Interpretation of Carbon-13-NMR-Spectra*; Heyden: London, U.K., 1976; pp 28−37.

(15) Agati, G.; Cerovic, G. Z.; Dalla Marta, A.; Di Stefano, V.; Pinelli, P.; Traversi, M. L.; Orlandini, S. Optically-assessed preformed flavonoids and suceptibility of grapevine to *Plasmopara viticola* under different light regimes. *Funct. Plant Biol.* **2008**, *35*, 77–84.

(16) Goetz, G.; Fkyerat, A.; Métais, N.; Kunz, M.; Tabacchi, R.; Pezet, R.; Pont, V. Resistance factors to grey mould in grape berries: identification of some phenolics inhibitors of *Botrytis cinerea* stilbene oxidase. *Phytochemistry* **1999**, *52*, 759–767.

(17) Khan, M. A.; Nabi, S. G.; Prakash, S.; Zaman, A. Pallidol, a resveratrol dimer from *Cissus pallida*. *Phytochemistry* **1986**, *25*, 1945–1948.

(18) Ohyama, M.; Tanaka, T.; Iinuma, M.; Goto, K. Two novel resveratrol trimers, leachianol-A and lachianol-B, from *Sophora lchiana*. *Chem. Pharm. Bull.* **1994**, *42*, 2117–2120.

(19) Snyder, S. A.; Zografos, A. L.; Lin, Y. Total synthesis of resveratrol-based natural products: a chemoselective solution. *Angew. Chem., Int. Ed.* **2007**, *46*, 8186–8191.

(20) Cichewicz, R. H.; Kouzi, S. A.; Hamann, M. T. Dimerization of resveratrol by the grapevine pathogen *Botrytis cinerea*. *J. Nat. Prod.* **2000**, *63*, 29–33.

(21) Takaya, Y.; Terashima, K.; Ito, J.; He, Y. H.; Tateoka, M.; Yamaguchi, N.; Niwa, M. Biomimic transformation of resveratrol. *Tetrahedron* **2005**, *61*, 10285–10290.

(22) Kulesh, N. I.; Veselova, M. V.; Fedoreev, S. A.; Denisenko, V. A. Polyphenols from *Vitis amurensis* stems. *Chem. Nat. Compd.* **2006**, *42*, 235–237.

(23) Oshima, Y.; Ueno, Y. Ampelopsin-D, ampelopsin-E, ampelopsin-H and *cis*-ampelopsin-E, oligostilbenes from *Ampelopsis brevipenduculata* var. Hancei roots. *Phytochemistry* **1993**, *33*, 179–182.

(24) Takaya, Y.; Yan, K. X.; Terashima, K.; Ito, J.; Niwa, M. Chemical determination of the absolute structures of resveratrol dimers, ampelopsins A, B, D and F. *Tetrahedron* **2002**, *58*, 7259–7265.

(25) Adesanya, S. A.; Nia, R.; Martin, M.-T.; Boukamcha, N.; Montagnac, A.; Pais, M. Stilbene derivatives from *Cissus quadrangularis*. *J. Nat. Prod.* **1999**, *62*, 1694–1695.

(26) Tanaka, T.; Iinuma, M.; Murata, H. Stilbene derivatives in the stem of *Parthenocissus quinquefolia*. *Phytochemistry* **1998**, *48*, 1045–1049.

(27) Niwa, M.; Ito, J.; Terashim, K.; Koizumi, T.; Takaya, Y.; Yan, K. X. (−)-Ampelopsin D is different from (−)-quadrangularin A. *Heterocycles* **2000**, *53*, 1475–1478.

(28) Li, X. C.; Ferreira, D. Stereoselective cyclization of stilbene derived carbocations. *Tetrahedron* **2003**, *59*, 1501–1507.

(29) Pryce, R. J.; Langcake, P. α-Viniferin: an antifungal resveratrol trimer from grapevines. *Phytochemistry* **1977**, *16*, 1452–1454.

(30) Langcake, P.; Pryce, R. J. The production of resveratrol and the viniferins by grapevine in response to ultraviolet irradiation. *Phytochemistry* **1977**, *16*, 1193–1196.

(31) Kurihara, H.; Kawabata, J.; Ichikawa, S.; Mishima, M.; Mizutani, J. Oligostilbenes from *Carex kobomugi*. *Phytochemistry* **1991**, *30*, 649–653.

(32) Suzuki, K.; Shimizu, T.; Kawabata, J.; Mizutani, J. New (3,5,4′)-trihydroxystilbene (resveratrol) oligomers from *Carex fedia* Nees var. *miyabei* (Franchet) T. Koyama (Cyperaceae). *Agric. Biol. Chem.* **1987**, *51*, 1003–1008.

(33) Barjot, C.; Tournaire, M.; Castagnino, C.; Vigor, C.; Vercauteren, J; Rossi, J. F. Evaluation of antitumor effects of two vine stalk oligomers of resveratrol on a panel of lymphoid and myeloid cell lines: comparison with resveratrol. *Life Sci.* **2007**, *81*, 1565–1574.

(34) Ito, J.; Niwa, M.; Oshima, Y. A new hydroxystilbene tetramer named isohopeaphenol from *Vitis vinifera* 'Kyohou'. *Heterocycles* **1997**, *45*, 1809–1813.

(35) Tanaka, T.; Itoa, T.; Nakaya, K.; Iinuma, M.; Riswan, S. Oligostilbenoids in stem bark of *Vatica rassak*. *Phytochemistry* **2000**, *54*, 63–69.

(36) Abe, N.; Ito, T.; Ohguchi, K.; Nasu, M.; Masuda, Y.; Oyama, M.; Nozawa, Y.; Ito, M.; Iinuma, M. Resveratrol oligomers from *Vatica albiramis*. *J. Nat. Prod.* **2010**, *73*, 1499–1506.

(37) Mattivi, F.; Reniero, F. Oligostilbenes from the roots of genus *Vitis*. *Bull. Liaison Groupe Polyphenols* **1992**, *16*, 116–118.

(38) Bavaresco, L.; Cantù, E.; Fregoni, M.; Trevisan, M. Constitutive stilbene contents of grapevine cluster stems as potential source of resveratrol in wine. *Vitis* **1997**, *36*, 115–118.

(39) Waffo-Teguo, P.; Lee, D.; Cuendet, M.; Merillon, J. M.; Pezzuto, J. M.; Douglas Kinghorn, A. D. Two new stilbene dimer glucosides from grape (*Vitis vinifera*) cell cultures. *J. Nat. Prod.* **2001**, *64*, 136–138.

(40) Pezet, R.; Gindro, K.; Viret, O.; Spring, J.-L. Glycosylation and oxidative dimerization of resveratrol are respectively associated to sensitivity and resistance of grapevine cultivars to downy mildew. *Physiol. Mol. Plant Pathol.* **2004**, *65*, 297–303.

(41) Pezet, R.; Gindro, K.; Viret, O.; Richter, H. Effects of resveratrol, viniferins and pterostilbene on *Plasmopara viticola* zoospore mobility and disease development. *Vitis* **2004**, *43*, 145–148.

(42) Gindro, K.; Spring, J. L.; Pezet, R.; Richter, H.; Viret, O. Histological and biochemical criteria for pbjective and early selection of grapevine cultivars resistent to *Plasmopara viticola*. *Vitis* **2006**, *45*, 191–196.

(43) Bavaresco, L.; Vezzulli, S.; Civardi, S.; Gatti, M.; Battilani, P.; Pietri, A.; Ferrari, F. Effect of lime-induced leaf chlorosis on ochratoxin A, *trans*-resveratrol, and ε-viniferin production in grapevine (*Vitis vinifera* L.) berries infected by *Aspergillus carbonarius*. *J. Agric. Food Chem.* **2008**, *56*, 2085–2089.

(44) Alonso-Villaverde, V.; Voinesco, F.; Viret, O.; Spring, J. L.; Gindro, K. The effectiveness of stilbenes in resistant *Vitaceae*: ultrastructural and biochemical events during *Plasmopara viticola* infection process. *Plant Physiol. Biochem.* **2010**, *49*, 265–274.

(45) Ha, D. T.; Chen, Q. C.; Hung, T. M.; Youn, U. J.; Ngoc, T. M.; Thuong, P. T.; Kim, H. J.; Seong, Y. H.; Min, B. S.; Bae, K. H. Stilbenes and oligostilbenes from leaf and stem of *Vitis amurensis* and their cytotoxic activity. *Arch. Pharm. Res.* **2009**, *32*, 177–183.